

Accepted refereed manuscript of:

Vives i Batlle J, Ulanovsky AV & Copplestone D (2017) A method for assessing exposure of terrestrial wildlife to environmental radon (Rn-222) and thoron (Rn-220), *Science of the Total Environment*, 605-606, pp. 569-577.

DOI: [10.1016/j.scitotenv.2017.06.154](https://doi.org/10.1016/j.scitotenv.2017.06.154)

© 2017, Elsevier. Licensed under the Creative Commons Attribution-NonCommercial-NoDerivatives 4.0 International
<http://creativecommons.org/licenses/by-nc-nd/4.0/>

1 **A method for assessing exposure of terrestrial wildlife to environmental**
2 **radon (^{222}Rn) and thoron (^{220}Rn)**

3 Jordi Vives i Batlle¹ (✉), Alexander Ulanovsky², David Coplestone³

4 ¹Belgian Nuclear Research Centre (SCK•CEN), Boeretang 200, 2400 Mol, Belgium. Tel: +32 (0)14
5 33 88 05, Fax: +32 (0)14 32 10 56, e-mail: jordi.vives.i.batlle@sckcen.be

6 ²Institute of Radiation Protection, Helmholtz Zentrum München – German Research Centre for
7 Environmental Health, Ingolstädter Landstraße 1, D-85764 Neuherberg, Germany

8 ³Faculty of Natural Sciences, University of Stirling, UK

9 **Abstract**

10 A method is presented to calculate radiation dose rates arising from radon, thoron and their
11 progeny to non-human biota in the terrestrial environment. The method improves on existing
12 methodologies for the assessment of radon to biota by using a generalised allometric approach
13 to model respiration, calculating dose coefficients for the ICRP reference animals and plants,
14 and extending the approach to cover thoron in addition to radon-derived isotopes. The method
15 is applicable to a range of environmental situations involving these radionuclides in wildlife,
16 with an envisaged application being to study the impact of human activities, which bring
17 NORM radionuclides to the biosphere. Consequently, there is a need to determine whether there
18 is an impact on non-human biota from exposure to anthropogenically enhanced radionuclides.

19 Keywords: radon; thoron; non-human biota; dose coefficients; International Commission on
20 Radiological Protection (ICRP)

21

22 Accepted for publication in *Science of the Total Environment* published by Elsevier.

23

24 **Introduction**

25 The radioactive isotopes $^{220,222}\text{Rn}$ appear in the environment as members of decay chains of
26 naturally occurring ^{232}Th and ^{238}U , thus having the historical names “thoron” and “radon”,
27 respectively.

28 Environmental radiological protection aims to ensure protection from anthropogenic sources of
29 radiation exposure, including those naturally occurring radionuclides (NORM) that might be
30 released into the environment due to human activity. Being of primordial origin, exposure to
31 radon isotopes and their radioactive progeny has been generally regarded as a background
32 exposure and deemed not relevant for radiation protection. However, naturally occurring
33 radionuclides such as radon isotopes $^{220,222}\text{Rn}$ and their radioactive progeny can give significant
34 exposure to terrestrial wildlife. For example, results show that absorbed dose rates to burrowing
35 mammals as a consequence of exposure to ^{222}Rn are likely to be at least one order of magnitude
36 higher than those suggested in previous evaluations of natural background exposure rates which
37 had omitted this radionuclide and exposure pathway (Beresford et al., 2012). The resulting dose
38 rates in some areas are considerably in excess of incremental no-effects benchmark dose rates
39 that have been suggested for use in screening levels (Beresford et al., 2012).

40 Unlike humans, various species are known to live in soil in close proximity to radon sources.
41 Their exposures to these naturally occurring radionuclides are often questioned. Moreover,
42 elevated levels of radon (^{222}Rn) and thoron (^{220}Rn) can appear in the environment as a result of
43 human activity, e.g. due to uranium mining, enrichment and processing, oil and gas production,
44 geothermal energy and water production, among others. Elevated activity concentrations of
45 TENORM (technologically enhanced naturally occurring materials), including radon and
46 thoron predecessors (^{232}Th and ^{238}U), can be regarded as anthropogenic sources of radiation
47 exposure. In such cases, human presence can be deliberately restricted or humans might not be
48 present anyway (for example in the oceans or underground), thus no public exposure concerns
49 could be raised for humans, but exposures to wildlife inhabiting such places can still be
50 questioned and may need to be assessed in the context of natural preservation and protection.
51 In other words, animals and plants inhabit places in immediate proximity to the sources of the
52 radioactive noble gases and, for them, radon and thoron with their progenies may become
53 (unlike for humans) potentially relevant radiologically.

54 Assessing doses of radiation exposure due to radon isotopes and their progeny commonly
55 appears as a difficult task due to complicated processes of radon effluence, build-up of

56 radioactive progeny, chemical forms and attachment to aerosols, intake, deposition and
57 retention of radon-related radioactivity in the body of living organisms. Only a few studies in
58 rodents consider the lung deposition of radon products using a model of the tracheobronchial
59 tree (Harley, 1988; Hofmann et al., 2006).

60 Due to complexity, radon dosimetry appeared for decades as a scientific challenge. Even for
61 humans, exposure to radon isotopes and their progeny is not covered by standard ICRP
62 biokinetic and dosimetric models (ICRP, 2010) and, correspondingly, no human dose
63 coefficients have been recommended by ICRP.

64 The diversity of non-human biota, expressed by their biological, morphological and metabolic
65 differences, makes radon dosimetry for wildlife an even more complex task than that for
66 humans. The problem is compounded by the shortage of studies dealing specifically with
67 methodologies for the calculation of radon and thoron doses to wildlife (most investigations are
68 orientated to human dosimetry or use laboratory animals as a surrogate for human exposures).

69 Laboratory rats particularly are used in inhalation studies as a surrogate for human exposures
70 and dosimetry models for inhaled radon progeny in the rat lung have been developed, with the
71 objective of predicting bronchial dose distributions (Harley, 1988; Hofmann et al., 2006; Strong
72 and Baker, 1996; Winkler-Heil et al., 2015). These models are quite complex, involving a full
73 model of the tracheobronchial tree and associated lung deposition, redistribution within the
74 airways and clearance processes for radon and thoron daughters. Such approaches are by
75 necessity biological species-specific and require a number of parameters that are not available
76 except for the laboratory animals studied. As such, they go beyond the need for a practical
77 assessment tool useable for radiological screening purposes, which has to be sufficiently
78 generic to cover a variety of terrestrial animals and must have an in-built level of conservatism
79 (approximately one order of magnitude) in order to be adequately robust.

80 Although the use of simplified and conservative methods for non-human biota appears as
81 rational and appropriate, there are very few methods for radon already being in use (MacDonald
82 and Laverock, 1998; Vives i Batlle et al., 2008). To our knowledge, no method has been
83 published to calculate doses to non-human biota as a result of exposure to thoron, but a method
84 has been developed for ^{41}Ar , $^{85,88}\text{Kr}$ and $^{131\text{m},133}\text{Xe}$ wildlife dose assessment (Vives Batlle et al.,
85 2015).

86 The radon approach by MacDonald and Laverock (1998) was designed for burrowing
87 mammals, although the equations have been adapted to calculate radiation doses for birds

88 (Kitowski et al., 2015). The method by Vives i Batlle et al. (2008), which has the advantage of
89 having a wider range of application for different terrestrial animal and plant species, was
90 initially developed in response to a need by the England and Wales Environment Agency to
91 improve on an earlier interim approach, so as to conduct a trial assessment with set ^{222}Rn
92 authorisation limits under the UK Radioactive Substances Act (RSA) 1993. The approach was
93 further developed as a dose assessment screening tool (Vives i Batlle et al., 2012), though it is
94 as yet to be integrated into the ERICA tool for radiological impact to non-human biota. It was
95 subsequently used in a study to derive exposures of burrowing mammals to ^{222}Rn (Beresford et
96 al., 2012), becoming the initial basis of the more detailed and widely applicable methodology
97 presented here.

98 This article deals with the issue of radon, thoron and progeny to non-human biota, providing a
99 bespoke allometric method to calculate dose rates to terrestrial wildlife. We have recalculated
100 the potential α -energy concentration (PAEC) for radon and thoron, following the dosimetric
101 approach adopted by ICRP and using the contemporary radionuclide emission data also
102 recommended by ICRP (ICRP, 2008b). Then, we deliver tables with conservative (assuming
103 full retention) estimates of dose coefficients (DCs) for non-human entities due to radon, thoron
104 and their progeny, covering both internal and external exposure situations. The presented DCs
105 illustrate the importance of having an appropriate definition of a critical organ (part of the body)
106 for internal exposure to radionuclides emitting non-penetrating radiation (α -particles) and show
107 that an implausible choice of the critical organ or tissue may lead to growth of uncertainty by
108 several orders of magnitude.

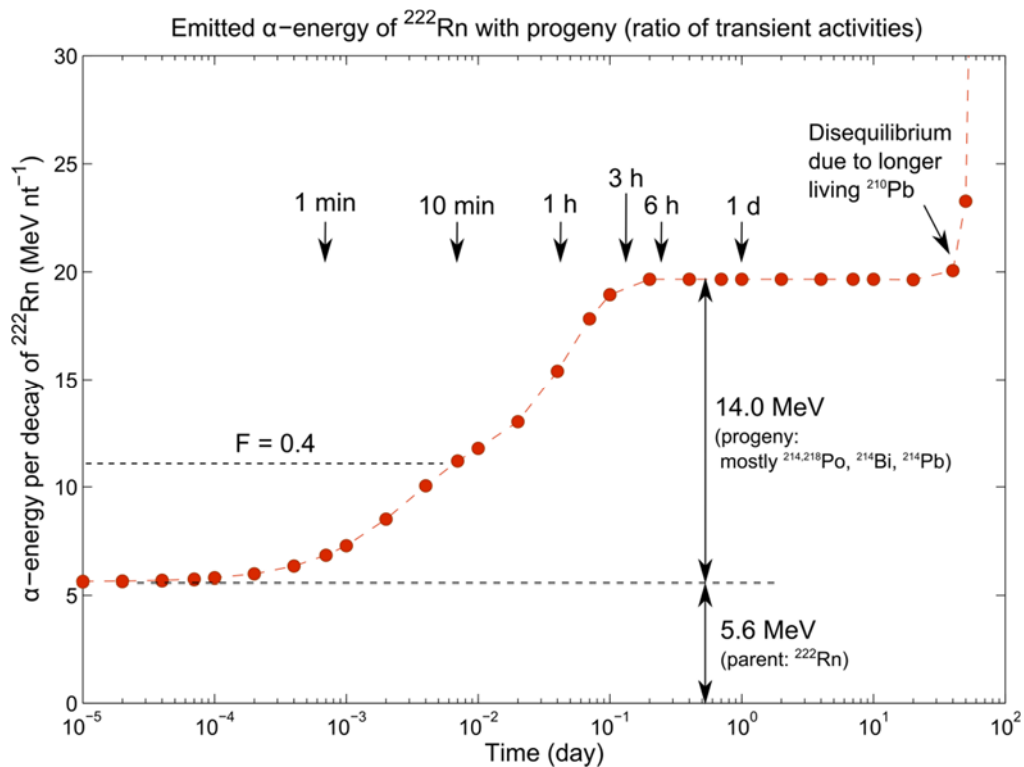
109 **Materials and methods**

110 **Main dosimetric properties of radon and thoron progeny**

111
112 The dosimetry of radon (^{222}Rn) and its daughter products is a widely considered topic, having
113 been the object of numerous ICRP publications (ICRP, 1987; ICRP, 1993; ICRP, 2010; ICRP,
114 2014b). Thoron (^{220}Rn), due to its shorter half-life, is usually neglected in assessments of human
115 indoor exposure, because of significant decay during transport from the point of origin to human
116 dwellings. However, assessment of radiation exposure of animals and plants living in direct
117 proximity to sources of radon gas may require accounting for contributions of radon as well as
118 of shorter-lived thoron.

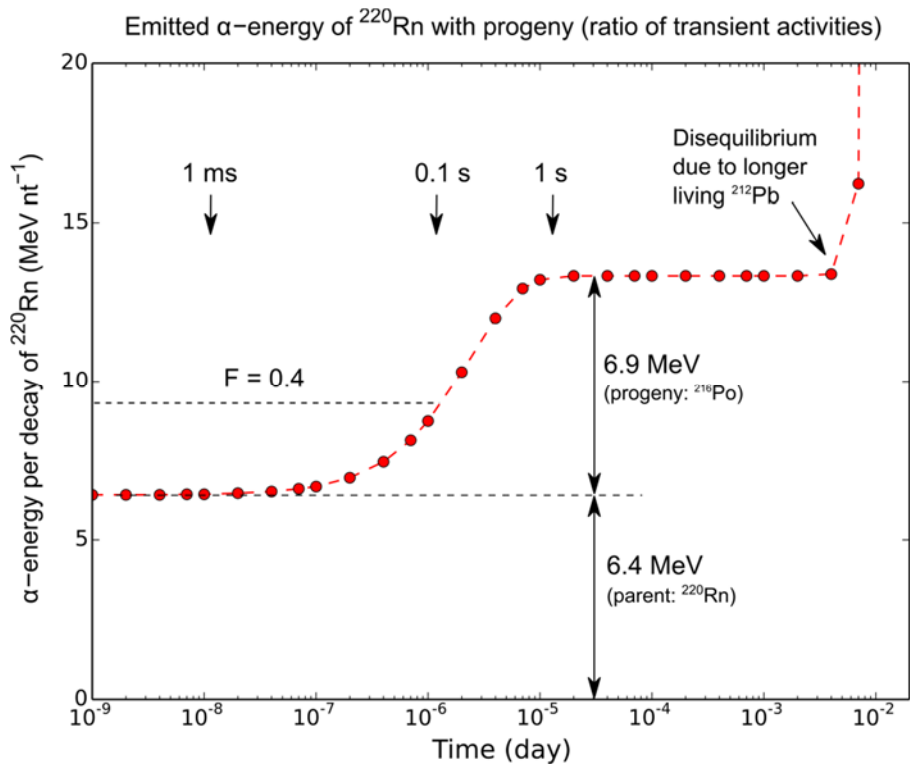
119 Figures 1 and 2 give the energies of α -particles emitted by radon isotopes and their progeny
120 accounted via the ratio of transient activities of daughter nuclides to that of the parent. From

121 the figures, the total α -energy emitted per single decay of the parent nuclide can be seen to vary
 122 within a factor of two (^{220}Rn) or three (^{222}Rn) for non-equilibrated mixtures of decay chain
 123 members. The value of the equilibrium factor $F = 0.4$ shown in the figures is commonly
 124 assumed in human dosimetry (Keller et al., 1984; Wenbin et al., 1990; Wrixon et al., 1988) and
 125 thus can be used as a plausible default value for exposure of terrestrial wildlife in the outdoor
 126 environment when experimentally-based information is missing. Correspondingly, $F = 1$ can
 127 be regarded as a conservative value. However, as seen from Figure 2, Thoron is a short-lived
 128 nuclide and, after reaching equilibrium with its daughter ^{216}Po in about 10 min, decays
 129 significantly, resulting in a highly non-equilibrium state with other progeny (^{212}Pb , ^{212}Bi , ^{212}Po ,
 130 and ^{208}Tl). Thus, estimates of biota exposure in this case may appear more realistic with an
 131 equilibrium factor equal to one.



132

133 Figure 1: Energy of α -particles emitted by radon (^{222}Rn) and its progeny per decay of the
 134 parent nuclide



135

136 Figure 2: Energy of α -particles emitted by thoron (^{220}Rn) and its progeny per decay of the parent
 137 nuclide

138 As seen in Figures 1 and 2, the use of transient activity ratios in expressing the total energy
 139 emitted by radioactive parent and daughter nuclides may be inconvenient for radon and simply
 140 impractical for thoron. For these decay chains, a ratio of time-integrated activities appears as a
 141 practical alternative compatible with the concept of potential α -energy, which is common for
 142 radon dosimetry (ICRP, 1993; Porstendörfer, 1994). However, computing time-integrated
 143 activity ratios requires assessment-specific data: exposure time and location factors. In this
 144 paper, a generic approach is presented, which conservatively assumes conditions of full
 145 equilibrium between the parent and the daughters. Although convenient and plausible in many
 146 practical situations, this generic assumption of equilibrium might however become invalid for
 147 certain assessment-specific time and location conditions.

148 **Assessment of internal exposures**

149 *Simplified representation of radon respiration*

150 For terrestrial animals and plants, the main pathway of internal exposure to radon and its
 151 progeny is respiration. The approach described here assumes conservatively full deposition and
 152 absorption of activity in respired air. Correspondingly, the DCs derived in the present study
 153 indicate upper bounds of radiation exposure due to environmental radon isotopes and their

154 progeny. DCs for internal radon exposure in the present study are formulated as aggregated
155 quantities, namely, per activity concentration in the ambient air, thus aggregating dose per unit
156 activity in the body and concentration ratio between activity in the body and in the ambient air.
157 This makes them different from the internal DCC definition adopted in the ICRP dosimetry
158 framework for non-human biota (ICRP, 2008a), which are formulated in terms of dose rate per
159 unit activity concentration in the body or organ. In other words, our formulation is
160 complementary to the ICRP approach, and can be regarded as conservative in the sense that it
161 can eliminate from consideration situations of low radiological relevance by calculating doses
162 that may be safely said to not have been exceeded. This can be regarded as a more practical and
163 convenient alternative in certain exposure situations.

164 Respiration of radon and its progeny is modelled as constant flow into the relevant respiratory
165 system, conservatively assuming that radon gas is in equilibrium with its daughters (equilibrium
166 factor $F = 1$), thus helping to avoid an underestimation of the dose due to a variety of
167 environmental conditions which may not be fully known at the time of assessment. The degree
168 of conservatism incurred by this equilibrium assumption does not typically exceed as factor of
169 2 or 3, because environmental measurements usually show the annual mean value of F in open
170 air to be 0.4 (Keller et al., 1984), 0.51 ± 0.12 (Kojima, 1996) or 0.6 (Wenbin et al., 1990).
171 Elsewhere (Porstendörfer, 1994), a range 0.4 – 0.8 at 1.5 m above ground was also reported.
172 Other authors (Beresford et al., 2012) applied an equilibrium factor for outdoor air of $F = 0.8$.

173 Full absorption of progeny is assumed within the respiratory organs/systems, and no further
174 redistribution of the deposited activity due to biokinetic processes, exhalation or excretion from
175 the organism, is accounted for. Parent radon isotopes are chemically inert gases and they are
176 assumed to escape without significantly contributing to the total internal dose. This is because,
177 although it can be present in physical solution, chiefly in the body water and fat, radon has a
178 small solubility in water and body fluids and, being chemically inert, it does not participate at
179 normal pressures in biochemical reactions of the human body (Tobias et al., 1949).

180 Under the above assumptions, the following equation applies to the conversion coefficient, DC
181 ($\mu\text{Gy h}^{-1} \text{Bq}^{-1} \text{m}^3$), which is defined as absorbed dose rate in target tissues due to radon progeny
182 per unit activity concentration of parent isotope (^{220}Rn or ^{222}Rn) in ambient air:

$$183 \quad DC = B \frac{E}{M_T} g \quad (1)$$

184 where B is the respiration (breathing) rate ($\text{m}^3 \text{h}^{-1}$), E is the total energy absorbed in the target
185 tissues due to radiation emitted by the radon progeny until decay to (quasi)stable lead isotopes
186 ($\mu\text{J Bq}^{-1}$), M_T is the mass of the target tissue/organ (kg), and g is the geometrical factor which
187 takes into account (in)homogeneity of activity deposition in airways/respiratory organs
188 (dimensionless).

189 Alpha-particles contribute about 95% to the total emitted energy of radon progeny (ICRP,
190 2008b) and this energy can be represented using concept of the potential α -energy (ICRP, 1987;
191 ICRP, 1993), thus assuming respiration of equilibrium mixture of radon daughters and
192 neglecting the contribution of electrons and photons to the absorbed dose. The reason for
193 neglecting the electron and photon contributions is not only the fact that they carry 5% or less
194 of the emitted energy, but also that they are more penetrating radiation types and their absorbed
195 fractions in the tissue of interest can be significantly less than one, depending on the organism
196 anatomy or morphology. Updated values of the potential α -energy, based on data from the
197 ICRP *Publication 107* (ICRP, 2008b), are shown in Table 1, which is functionally similar to
198 the previously published Table A1 in ICRP *Publication 50* (ICRP, 1987) and Table 2 in
199 *Publication 65* (ICRP, 1993).

200 Due to short range of α -particles in tissue, they can be regarded as non-penetrating and fully
201 depositing their energy in the tissue. In other words, absorbed fractions for α -particles are
202 assumed equal to one ($AF_\alpha \cong 1$) and the total α -energy released in decay of radon progeny is
203 assumed to be absorbed internally. The geometric factor g accounts for the heterogeneity of the
204 airways of some organisms, which might result in energy deposition not in the living tissues
205 but in internal air or in mucous or other inert biological fluids. Simple reasoning leads to the
206 conclusion that the geometrical factor may vary from 0.5 (α -emitters on interface) to 1.0 (α -
207 emitters deep in tissue).

208

209 Table 1: Potential α -energy for radon (^{222}Rn) and thoron (^{220}Rn) progeny calculated using
 210 emission data from ICRP *Publication 107* (ICRP, 2008b)

Radionuclide	Half-life	Potential α energy			
		per atom		per unit of activity	
		(MeV)	(10^{-12} J)	(MeV Bq $^{-1}$)	(10^{-10} J Bq $^{-1}$)
Radon (^{222}Rn) progeny					
^{218}Po	3.10 min	13.95	2.23	3743	6.0
^{214}Pb	26.8 min	7.84	1.26	18176	29.1
^{214}Bi	19.9 min	7.84	1.26	13496	21.6
^{214}Po	164.2 μs	7.84	1.26	1.9×10^{-3}	3.0×10^{-6}
Total (at equilibrium), per Bq of radon				35415	56.74
Thoron (^{220}Rn) progeny					
^{216}Po	0.145 s	15.86	2.54	3.318	5.3×10^{-3}
^{212}Pb	10.64 h	8.95	1.43	494807	792.7
^{212}Bi	60.55 min	8.95	1.43	46931	75.2
^{212}Po	3.0×10^{-7} s	8.95	1.43	2.5×10^{-6}	4.0×10^{-9}
Total (at equilibrium), per Bq of thoron				542047	870.73

211

212 The target tissue exposed by the radon progeny varies significantly depending on the physico-
 213 chemical properties of inhaled radon and its radioactive progeny, as well as on the biological
 214 variety of breathing organisms. For most types of organisms though, since the internal dose rate
 215 is predominantly due to α -radiation, the lungs will receive virtually the entire internal dose rate.
 216 A convenient assumption is that the sensitive tissues of the respiratory system have a cylindrical
 217 shape, since they consist of the epithelium surrounding the walls of the airways, as is the case
 218 for humans (Hofmann and Winkler-Heil, 2015; ICRP, 1994; ICRP, 2002). The most significant
 219 difference between human and rat lungs, in fact, is the branching structure of the bronchial tree,
 220 which is relatively symmetric in humans, but monopodial in rats (Winkler-Heil et al., 2015).
 221 Thus, assuming that the shape of the airways is a cylinder with radius R_{aw} and accounting for
 222 the small thickness h_T of the sensitive tissue ($h_T \ll R_{aw}$), we can express the mass of target
 223 tissues M_T as:

224
$$M_T = \rho_T S_T R_{aw} \left(\frac{h_T}{R_{aw}} + \frac{h_T^2}{2R_{aw}^2} \right) \approx \rho_T S_T h_T \quad (2)$$

225 where ρ_T is the density of the target tissue taken equal to 10^3 kg m^{-3} , and S_T is the
226 tracheobronchial surface area (m^2).

227 The active depth of sensitive tissue, i.e. the thickness of the bronchial epithelium (without cilia),
228 is assumed conservatively (for lack of species-specific information) to be $55 \text{ }\mu\text{m}$ as for the ICRP
229 human respiratory tract model (ICRP, 1994).

230 *Allometric scaling of respiration parameters for animals*

231 The respiratory tract properties, including breathing rate, vary among organisms because of
232 their biological and morphological diversity. Despite this variability, there exist structural
233 similarities between related organisms; these similarities are expressed by so-called allometric
234 relationships or ‘laws’ (Kleiber, 1947; Rubner, 1883). Allometric scaling can be used to assess
235 organism-specific parameters. For example, in mammals, the breathing rate has been found to
236 correlate with body mass M according to the following allometric equation:

237
$$B(M) = a M^b \quad (2)$$

238 where a and b are the base and exponent, the latter being close to $3/4$, according to Kleiber’s
239 allometric scaling law (Kleiber, 1932; Kleiber, 1947). For example, cardiac output and
240 pulmonary exchange scale as $M^{3/4}$ in mammals (Schmidt-Nielsen, 1984), and similarly for the
241 rate of respiratory ventilation (West and Brown, 2005). However, the above equation is an
242 approximation, and experimental data suggest that the relationship between mass and metabolic
243 rate has convex curvature on a logarithmic scale (Kolokotronis et al., 2010). This means that
244 extrapolating the breathing rate as a function of body mass using Eq. 2 from either small or
245 large masses will result in an underestimation at the opposite end of the mass range.

246 This problem can be rectified by using generalised allometric equations (ICRP, In press;
247 Ulanovsky, 2016). For example, for the breathing rate of terrestrial mammals, the generalised
248 allometric equation is as follows:

249
$$B(M) = a^* M^{b^*} = e^{\beta_0} M^{1+\beta_1+\beta_2 \ln M}, \quad (3)$$

250 where B is the ventilation rate ($\text{m}^3 \text{ h}^{-1}$) and M is the mass of the organism (kg).

251 From the compilation of Bide et al. (2000) on ventilation rate for terrestrial mammals, the
252 following values have been found statistically significant (Ulanovsky, 2016): $\beta_0 = -3.562 \pm$

253 0.050, $\beta_1 = -0.226 \pm 0.019$ and $\beta_2 = (7.26 \pm 4.45) \times 10^{-3}$. Note that neglecting the log-quadratic
 254 term in exponent reduces eq. (3) to:

255
$$B(M) = e^{\beta_0} M^{1+\beta_1},$$

256 which is simply the ‘Kleiber law’ with an exponent of 0.77 instead of 0.75. In this sense, Eq.
 257 (3) can be called a generalisation of the first-order allometric equation.

258 Using the respiratory tract parameters of the ICRP ‘Reference Man’ (ICRP, 2002) and applying
 259 allometric scaling, the DCs for internal exposure of animals (terrestrial mammals) can be
 260 expressed as simple allometric power functions for a range of target tissues such as, for
 261 example, the bronchial epithelium (B), tracheobronchial tree (TB), full lung (L) and whole body
 262 (WB):

263
$$DC_B = \frac{E}{\rho_T h_T S_B^{RM}} \left(\frac{M_{RM}}{M} \right)^{\frac{2}{3}} B(M) \quad (4)$$

264
$$DC_{TB} = \frac{E}{\rho_T h_T S_{TB}^{RM}} \left(\frac{M_{RM}}{M} \right)^{\frac{2}{3}} B(M) \quad (5)$$

265
$$DC_L = \frac{E}{a_L M^{b_L}} B(M) \quad (6)$$

266
$$DC_{WB} = \frac{E}{M} B(M) \quad (7)$$

267 Where a_L and b_L are the base and exponent of the allometric formulae for lung mass (Vives i
 268 Batlle et al., 2012), $S_{TB}^{RM} = 0.269$ (m²) and $S_B^{RM} = 0.0291$ (m²) are the surface area of the
 269 tracheobronchial tree and the bronchial epithelium of the ICRP Reference Man, and $M_{RM} = 70$
 270 kg is the mass of the ICRP Reference Man.

271 The above approach is derived for terrestrial mammals. Thus, there is no guarantee that
 272 respiration rates of other lung-breathing ICRP reference organisms such as birds, reptiles and
 273 amphibians still follow Eq. 3 for the breathing rate or the other allometric relationships for
 274 respiratory system implicitly present in Eqs. 5-7. As a practical solution, Vives i Batlle et al.
 275 (2012) have suggested that the allometric approach for mammals could be used conjecturally
 276 for organisms having structurally simpler breathing systems if no other option is available, and
 277 that this is likely to give conservative estimates for these organisms.

278 *Internal exposure of plants*

279 For plants, a simple conservative approximation is used, whereby the whole surface area of the
280 plant is assumed to be exchanging gases with the atmosphere and the following approximations
281 for DCs of plant tissue (DC_S) and whole plant (DC_P) have been suggested (Vives i Batlle et al.,
282 2012):

$$283 \quad DC_S = E \frac{a_{PL} a M^{b_{PL}-1}}{2\sqrt{6}h_T} \quad (8)$$
$$DC_P = E a_{PL} M^{b_{PL}-1}$$

284 where $a_{PL}=1.95 \times 10^{-4}$ ($\text{m}^3 \text{s}^{-1}$) is the allometric base for respiration rate in plants calculated
285 based on net CO_2 efflux data by Vives i Batlle et al. (2012) and previous data (Reich et al.,
286 2005), and b_{PL} is the exponent of that allometric breathing rate, which for plants is calculated
287 to be very close to unity at 1.02 (Vives i Batlle et al., 2012) so that Eq. 8 is virtually mass-
288 independent. Moreover, a is the minor axis or average of non-equal minor axes of the ellipsoid
289 representing the plant (m), h_T is the depth of sensitive tissue, which is based on the morphology
290 of plant cells and the range of α -particles in plant tissue, whereupon the representative value of
291 the depth of sensitive tissue can be taken to be 50 μm .

292 It should be noted also that due to the important role of carbon dioxide in the metabolism of
293 living species, the allometric approximation for the plant respiration rate in Eq. 8 may lead to
294 additional conservatism of the aggregated DCs.

295 Due to its simplicity, the above approximation has been tested against a more complex dynamic
296 model that considers interception of the unattached and attached fractions of the airborne radon
297 daughters by plant stomata, diffusion of radon gas through stomata, permeation through the
298 plant's epidermis and uptake of deposited activity to the plant interior (Vives i Batlle et al.,
299 2011). This more sophisticated approach can calculate separately the dose contributions arising
300 from radioactive materials deposited internally, externally and on the plant surface.

301 Results of this comparison are given in Table 8 of Vives i Batlle *et al.* (2011). The total (internal
302 plus surface-deposition) dose rates for the present methodology are 18% lower than calculated
303 by the plant dynamic model, which is reasonably consistent. External dose rates for the current
304 approach are 1.9 times higher than the plant model, which is not surprising, given that we
305 adopted an equilibrium factor of 1, whereas the dynamic model generates an equilibrium factor
306 for outdoor air of about 0.5.

307 **Assessment of external exposures**

308 *Absorbed fractions and DC approach for animals and plants*

309 External exposure of terrestrial animals and plants to radon isotopes and their progeny may
310 occur in various locations: in soil, on the ground surface and in the air above. Due to the short
311 range of α -particles even in air, external exposure to radon isotopes and their progeny is mainly
312 created by photons and electrons emitted by ambient radioactive sources.

313 Under the assumptions of a uniform isotropic model, external exposure can be considered as
314 complementary to internal and, correspondingly, it can be expressed via absorbed fractions for
315 specific radiation types and for the given shapes of the body (Ulanovsky and Prohl, 2012).

316 The external dose assessment methodology adopted here allows expressing the DC for external
317 exposure of terrestrial animals in soil and on the surface to sources distributed in soil, as well
318 as for organisms above the ground interface exposed to sources in soil or in air. Being flexible
319 and versatile, this approach is based on the dataset calculated by Monte Carlo technique for a
320 set of pre-defined shapes corresponding to FASSET/ERICA organisms (Taranenko et al., 2004)
321 and for tissue-equivalent spheres (Ulanovsky, 2014) for terrestrial organisms on and above
322 ground surface exposed to radioactive sources in soil or in air. The DC for external exposure of
323 terrestrial organisms can be interpolated for arbitrary masses and heights above ground, though
324 obviating the effects of shape.

325 An alternative analytical parameterisation had been suggested based on a set of absorbed
326 fractions for pre-defined set of shapes representing various aquatic and terrestrial animals
327 (Vives i Batlle et al., 2004). Absorbed fractions for these shapes have been calculated using
328 Monte Carlo integration of point kernels for photons and electrons (Berger, 1968; Berger,
329 1971). Correspondingly, these approximations for absorbed fractions have been applied to
330 compute DCs for terrestrial animals exposed to radon and progeny isotopes in air. This
331 approach accounted for the short-lived progeny of ^{222}Rn included ^{218}Po , ^{218}At , ^{214}Pb , ^{214}Bi and
332 ^{214}Po . Longer-living, quasi-stable ^{210}Pb and its progeny ^{210}Bi and ^{210}Po have been ignored.
333 Radiations emitted by the considered nuclides encountered 93 electron-, 75 gamma- and six α -
334 lines, for which values for the decay energy or mean energy and the related quantum yields
335 were taken from the ICRP Publication 38 (ICRP, 1983).

336 External exposure to α -particles is commonly ignored because of their short range and the
337 shielding properties of tissue layers (e.g. fur, feather or dead skin) which cover the bodies of
338 organisms. The contributions of low-energy ($E < 10$ keV) electrons and photons sources to the
339 external DC have been found negligible in comparison with electrons and photons of higher
340 energy.

341

342 **Results and discussion**343 **Dose coefficients for internal exposure**

344 Calculated radon and thoron DCs for some ICRP Reference Animals and Plants (RAP) are
 345 given in Tables 2 and 3. The calculation of internal absorbed dose can be carried out simply by
 346 multiplying the listed DCs by the parent radon activity concentration in ambient air. A linear
 347 correction factor can be applied if an equilibrium factor different from unity is required.

348 Table 2: Parameters for calculation and values of aggregated unweighted DCs for internal
 349 exposure of animals due to progeny of radon isotopes $^{220,222}\text{Rn}$

Parameter or quantity	Amphibian (ICRP Frog) ^a	Reptile (ERICA snake) ^a	Mammal small (ICRP rat)	Mammal big (ICRP deer)	Bird (ICRP duck) ^a
M (kg)	0.0314	0.744	0.314	245	1.26
a (m)	0.08	1.2	0.2	1.3	0.3
b (m)	0.03	0.035	0.06	0.6	0.1
c (m)	0.025	0.035	0.05	0.6	0.08
B ($\text{m}^3 \text{h}^{-1}$)	2.1×10^{-3}	0.023	0.012	2.5	0.034
DCs per air concentration of ^{222}Rn ($\mu\text{Gy h}^{-1} \text{Bq}^{-1} \text{m}^3$)					
DC_B	1.4	1.8	1.7	4.2	1.9
DC_{TB}	0.15	0.20	0.18	0.46	0.21
DC_L	0.032	0.014	0.017	4.1×10^{-3}	0.012
DC_{WB}	3.8×10^{-4}	1.7×10^{-4}	2.1×10^{-4}	5.8×10^{-5}	1.5×10^{-4}
DCs per air concentration of ^{220}Rn ($\mu\text{Gy h}^{-1} \text{Bq}^{-1} \text{m}^3$)					
DC_B	22	28	26	65	30
DC_{TB}	2.4	3.0	2.8	7.0	3.2
DC_L	0.49	0.21	0.26	0.062	0.18
DC_{WB}	5.9×10^{-3}	2.6×10^{-3}	3.2×10^{-3}	8.9×10^{-4}	2.4×10^{-3}

^aDC for non-mammals are shown for illustrative purposes only

350

351 Table 3: Parameters for calculation and values of aggregated unweighted DCs for internal
 352 exposure of plants due to progeny of radon isotopes $^{220,222}\text{Rn}$

Parameter or quantity	Lichen & bryophytes (ICRP bryophyte)	Grasses and herbs (ICRP wild grass)	Trees (ICRP pine tree)
M (kg)	1.1×10^{-4}	2.6×10^{-3}	471
a (m)	0.04	0.05	10
b (m)	2.3×10^{-3}	0.01	0.3
c (m)	2.3×10^{-3}	0.01	0.3
B ($\text{m}^3 \text{h}^{-1}$)	6.5×10^{-5}	1.6×10^{-3}	360
DCs per air concentration of ^{222}Rn ($\mu\text{Gy h}^{-1} \text{Bq}^{-1} \text{m}^3$)			
DC_{SS}	0.031	0.14	5.5
DC_{WB}	3.3×10^{-3}	3.5×10^{-3}	4.5×10^{-3}
DCs per air concentration of ^{220}Rn ($\mu\text{Gy h}^{-1} \text{Bq}^{-1} \text{m}^3$)			
DC_S	0.48	2.2	85
DC_P	0.051	0.054	0.069

353

354 Alpha-particles belong to class of densely ionising high-LET radiations. Correspondingly, an
 355 assessment of the radiobiological effects of exposure to radon might require weighting internal
 356 doses with an appropriate radiation weighting factor for α -particles (W_α). For human
 357 radiological protection, ICRP recommends using a value of 20 for the W_α (ICRP, 2007), whilst
 358 for non-human biota, where protection of a species is aimed at the population level and radiation
 359 weighting factors need to be formulated for biological endpoints that could “lead to changes in
 360 population size or structure” (ICRP, 2014a), there is no recommended value yet. Although a
 361 degree of consensus around a value of $W_\alpha = 10$ has emerged (Brown et al., 2008; Vives i Batlle
 362 et al., 2004), the DCs presented in this article are left un-weighted to avoid loss of generality.

363 The present approach is compatible with the earlier method of MacDonald and Laverock
 364 (1998), except that these authors considered the whole lung as reference tissue for dose
 365 calculation. For non-penetrating α -particles, a simple re-scaling procedure can be used to
 366 compare the dose for different reference tissues to the dose to a whole lung as calculated by

367 McDonald and Laverock (1998). Previous comparison (Vives i Batlle et al., 2012) showed the
368 compatibility of the dose rates obtained by both methods.

369 As seen in Table 2, DCs for animals vary within four orders of magnitude between
370 compartments of respiratory tract and the whole body. In real exposure situations, air contains
371 the radioactive progeny in gaseous form and attached to aerosols and dust. Depending on the
372 size of aerosol particles and their chemical form, deposition and further absorption of
373 radioactive substances in airways may vary significantly, thus leading to various patterns of
374 activity distribution between different parts of respiratory system and other organs. Due to this,
375 it appears plausible to assume that more realistic dose estimates can be achieved by assuming
376 fractional deposition in various compartments and, correspondingly, by computing the total
377 internal dose as the weighted sum of partial doses in the compartments.

378 As previously stated, the DCs for amphibians, birds and reptiles are to be used conjecturally
379 because the respiratory systems of these animals are not only dimensionally but also structurally
380 different. DC values are given here for illustrative purposes and are not guaranteed for use in
381 assessments until allometric modelling of the respiration rates for these organisms is established
382 on a sounder basis.

383 The DCs shown above are given for various target tissues, while the whole body dose is the
384 quantity most often used in assessments of environmental risk, including previous radon studies
385 (Beresford et al., 2012; Vives i Batlle et al., 2008). This is due to scarcity of data on radiation
386 effects in wild animals and plants with which the predicted dose rates to target tissues could be
387 interpreted. The dose-rate benchmarks used by ICRP are based primarily on whole-body
388 exposures (ICRP, 2008a).

389 *Calculated external DC values*

390 The DCs for the ICRP RAPs in the terrestrial environment exposed to external sources of radon
391 and thoron isotopes and their progenies in the ambient air are given in Table 4. The data shown
392 in the table come from two independent methods. The first method (Vives i Batlle et al., 2012)
393 under assumptions of uniform isotropic model computes DCs for external exposure as
394 complementary fractions to the full absorption limit. An analytical approximation, based on
395 Monte-Carlo-integrated point kernels of various radiation in an infinite medium, is used for
396 computation of absorbed fractions for photons and electrons. Further re-scaling of the computed
397 DC, using density of air at normal conditions, allowed expressing the DC as per unit volume
398 activity concentrations in air.

399

400 Table 4: Comparison of the DC for animals and plants externally exposed to radon and thoron
 401 ($^{220,222}\text{Rn}$) and their progeny in ambient air

Organism	DC ($\mu\text{Gy h}^{-1} \text{Bq}^{-1} \text{m}^3$)			
	in infinite air ^a	in air ^b ($h = 500$ m)	in air ^b ($h = 10$ m)	on the ground ^b
Radon (^{222}Rn) and progeny				
Amphibian (ICRP frog)	7.8×10^{-4}	7.5×10^{-4}	4.4×10^{-4}	4.1×10^{-4}
Reptile (FASSET snake)	7.6×10^{-4}	7.5×10^{-4}	4.4×10^{-4}	4.1×10^{-4}
Mammal (ICRP rat)	7.3×10^{-4}	7.6×10^{-4}	4.5×10^{-4}	4.1×10^{-4}
Mammal (ICRP deer)	3.8×10^{-4}	5.1×10^{-4}	3.0×10^{-4}	2.8×10^{-4}
Bird (ICRP duck)	6.9×10^{-4}	7.5×10^{-4}	4.4×10^{-4}	4.1×10^{-4}
Lichen and bryophytes (ICRP bryophytes)	9.9×10^{-4}	6.0×10^{-4}	3.5×10^{-4}	3.3×10^{-4}
Grasses and herbs (ICRP wild grass)	8.5×10^{-4}	7.2×10^{-4}	4.2×10^{-4}	3.9×10^{-4}
Tree (ICRP pine tree)	5.1×10^{-4}	4.5×10^{-4}	2.7×10^{-4}	2.5×10^{-4}
Thoron (^{220}Rn) and progeny				
Amphibian (ICRP frog)	n.a.	6.7×10^{-4}	4.0×10^{-4}	3.8×10^{-4}
Reptile (FASSET snake)	n.a.	6.9×10^{-4}	4.1×10^{-4}	3.9×10^{-4}
Mammal (ICRP rat)	n.a.	6.9×10^{-4}	4.2×10^{-4}	3.9×10^{-4}
Mammal (ICRP deer)	n.a.	4.9×10^{-4}	3.0×10^{-4}	2.8×10^{-4}
Bird (ICRP duck)	n.a.	6.9×10^{-4}	4.1×10^{-4}	3.9×10^{-4}
Lichen and bryophytes (ICRP bryophytes)	n.a.	4.5×10^{-4}	2.7×10^{-4}	2.5×10^{-4}
Grasses and herbs (ICRP wild grass)	n.a.	6.0×10^{-4}	3.6×10^{-4}	3.5×10^{-4}
Tree (ICRP pine tree)	n.a.	4.4×10^{-4}	2.7×10^{-4}	2.5×10^{-4}

402 ^aUniform isotropic model method, using absorbed fractions based on Monte Carlo integration of photon
 403 and electron point kernels (Vives i Batlle et al., 2012)

404 ^bAbsorbed doses in tissue-equivalent spheres exposed to photon-only sources in air (Ulanovsky, 2014)

405

406 The second method (Ulanovsky, 2014) uses differential air kerma above infinite terrain due to
407 radioactive sources in ambient air, calculated by a Monte Carlo method. Absorbed doses for
408 living species have been derived from the differential air kerma using a dose-per-kerma
409 conversion function, which is interpolated using data pre-computed by an analogue Monte
410 Carlo method for tissue-equivalent spheres in isotropic monoenergetic photon fields. The
411 results obtained with this method are provided for both radioactive radon isotopes ($^{220,222}\text{Rn}$)
412 and their progeny.

413 The method based on the uniform isotropic model has been compared with the external DC for
414 in-soil exposure to radon and progeny using a DC calculation facility (Ulanovsky et al., 2008)
415 largely compatible to that available in the ERICA assessment tool (Brown et al., 2016; Brown
416 et al., 2008). The comparison was satisfactory, with relative differences ranging from 3 to 10%
417 in animals and 3 to 25% in plants. These differences are attributable to differences in the way
418 the absorbed fractions are calculated by the two methods.

419 The comparison of the DC for animals and plants externally exposed to radon isotopes given in
420 Table 4 demonstrates (a) good compatibility regardless of different methods and data used in
421 their computations, (b) low inter-species variability of the external DC, and (c) variability of
422 the DC due to change of exposure source from infinite to semi-space, predictably limited within
423 a (geometrical) factor two. The low variability of the presented DC due to organism size and
424 irradiation geometry implies that the effect of transient activities in the radon and thoron decay
425 chains may become considerably stronger and more influential to dose estimates. As the DCs
426 in Table 3 are computed assuming equilibrium conditions in the decay chains, they can be
427 regarded as conservative estimates of the respective DCs resulting in non-equilibrated mixtures
428 of radon isotopes and their progeny.

429 *External dose calculation*

430 Assessment of external exposures of terrestrial biota to environmental radon and its progeny
431 should consider mobility of the radioactive gases and aerosols, which results in the existence
432 of various configurations of radioactive sources and biological targets. The variability of
433 habitats and life styles of biota also contribute to the variability of possible exposure scenarios.
434 The universal method to cope with this diversity is to apply the superposition principle, which
435 means that dosimetric response to a complicated (realistic) exposure scenario can be
436 characterised as a weighted sum of responses to simple basic exposure situations, for which the
437 DCs are already known or can be easily derived. Weighting of a basic scenario is expressed via
438 so-called 'occupancy factor', which is constructed to express: (a) the time-share spent by the

439 organism in locations described by the basic ‘source-target’ configurations (e.g. in soil, on the
440 ground surface, in air), and (b) the relative contribution of radiation sources affecting the
441 organism at the specified location.

442 An example of applying the occupancy factors in an external dose assessment can be given for
443 the situation where the organism is exposed to radiation arising from (a) radon present in the
444 air-filled soil pores (e.g. in burrows) and (b) direct immersion in the atmosphere with radon and
445 its progeny. Both components of the external dose can be represented by the following
446 equations:

$$447 \quad D_S = DC_{ext} \frac{C_{Rn}^s}{CF} F(f_S + 0.5f_{SS} + r_f f_A) \quad (9)$$
$$D_I = DC_{ext} C_{Rn}^a F(f_A + 0.5f_{SS})$$

448 where D_S and D_I ($\mu\text{Gy h}^{-1}$) represent the dose rates from radon in the air-filled soil pores and
449 direct immersion in the atmosphere, respectively; C_{Rn}^s (Bq kg^{-1}) is the concentration of ^{222}Rn
450 in soil, C_{Rn}^a (Bq m^{-3}) is the concentration of ^{222}Rn in atmospheric air, CF ($\text{m}^3 \text{kg}^{-1}$) is the factor
451 used to convert volume concentration of radon in the air of the soil pores to mass concentration
452 of radon in soil, accounting for soil porosity, DC_{ext} ($\mu\text{Gy h}^{-1} \text{Bq}^{-1} \text{m}^3$) is the DC, f_S , f_{SS} and f_A
453 (dimensionless) represent the occupancy factors for three exposure situations: below ground in
454 soil, on the soil surface and immersion in air above the ground, and F is the equilibrium factor
455 (if a value different from 1 is used). A dimensionless radiation-dependent reduction factor can
456 optionally be introduced to modify the dose for organisms in above-ground air as received from
457 radiation sources in soil. It is zero for α -particles and low-energy electrons and approximately
458 0.25 for higher energy electrons and photons.

459 It is not possible to give a CF value for all soils of different characteristics under varying
460 moisture conditions. By way of example, an indicative value for the CF of $10^{-4} \text{m}^3 \text{kg}^{-1}$ can be
461 obtained by assuming that radon in pore air is at the same concentration as ground level air
462 concentrations. This can be calculated as follows: The effective porosity of soil typically varies
463 within the ranges 0.01 - 0.18 for clay and 0.16 - 0.46 for medium sand (McWorter and Sunada,
464 1988). In wet soil, a portion of the available pore space will be occupied by water. An
465 assumption is made for free air space of 0.15 by volume. Assuming also a bulk density for soil
466 of 1500kg m^{-3} , the free air space would be $0.15/1500$ or $10^{-4} \text{m}^3 \text{kg}^{-1}$. Thus, this value can be
467 used as a conversion factor between activity concentration in air (Bq m^{-3}) and in wet soil (Bq
468 kg^{-1}).

469 Occupancy factors can be set as, for example, default values in the ERICA assessment tool
470 (Brown et al., 2016; Brown et al., 2008), which for terrestrial animals assumes 100% occupancy
471 on the soil surface except for rat which is considered to have 100% occupancy inside the soil.

472 *Uncertainties in dose calculation*

473 The methodology presented here is based on calculated dose coefficients, which as such cannot
474 be validated against direct measurement. However, it is possible to evaluate the uncertainties
475 in the dose calculation process. On the one hand, the analytical approximation used to calculate
476 absorbed fractions with body shapes from spherical to highly protracted or oblate ellipsoids has
477 an uncertainty (expressed by an absolute coefficient of variation) not exceeding 15% for
478 photons and 10% for electrons (Ulanovsky, 2014; Ulanovsky and Prohl, 2006; Ulanovsky et
479 al., 2008). On the other hand, the second-order polynomial formula used to estimate the
480 breathing rate as a function of organism mass (Eq. 3) has a low uncertainty of the residuals
481 characterised by a geometric standard deviation of 1.47, corresponding to a ratio of 97.5% to
482 2.5% percentiles being equal to approximately 4.6. The differences between absorbed whole
483 body dose and air kerma for the energies and organism sizes involved are also negligible, such
484 that the latter can serve as a reasonable surrogate for the average whole-body absorbed dose
485 (ICRP, In press). Ultimately, the numerical factors influencing our Monte Carlo-calculated DCs
486 are not the main uncertainty sources for exposure scenarios and attention should focus on other
487 more significant aspects of Eq. 9, such as the determination of contamination of the
488 environment in specific locations, the CR used to convert activity concentration between soil
489 and air, the equilibrium factor F and the occupancy factors used in the assessment.

490 **Conclusions**

491 A method has been presented to calculate radiation dose rates arising from radon and thoron
492 progenies to a selection of terrestrial biota represented by the ICRP Reference Animals and
493 Plants. This method is relatively simplified in terms of assuming spherical and ellipsoidal
494 geometries, uniform distribution of radionuclides in the biota, absorbed doses averaged to the
495 level of the whole organism, etc.

496 That radon or thoron and their progeny are natural sources of radiation is not a real argument
497 to neglect them in an impact assessment for wildlife, especially given the releases of
498 radioactivity from the industrial or technological applications resulting in enhanced
499 concentrations of NORM in the biosphere. These may be 'natural' isotopes but man artificially

500 introduces them in significant quantities in the surface environment and one should have
501 methods to deal with their radiological impact on non-human biota.

502 The implications of the contribution that $^{220,222}\text{Rn}$ makes to wildlife dose rates and effects
503 arising thereof, needs to be further explored with reference to the application of the ICRP
504 derived consideration reference levels (DCRLs) for wildlife (ICRP, 2008a) and other suggested
505 benchmark dose rates. The problem is compounded by the fact that data on radiation effects
506 arising from exposure of radon or thoron to biota are not currently available. Hence, this study
507 represents a start for enabling a future examination of the consequences of radon exposure and
508 subsequent comparisons with exposure to background (radon) levels, signalling the way for
509 future investigations.

510 **Acknowledgements**

511 The present work was carried out under the auspices of the International Commission on
512 Radiological Protection (ICRP) and its Committee 5 “Protection in the Environment” in
513 connection to activities of the ICRP Task Group 74 “More Realistic Dosimetry for Non-human
514 Species”.

515

516

517

518

519

520

521

522

523 **References**

- 524 Beresford N, Barnett C, Vives i Batlle J, Potter ED, Ibrahim Z-F, Barlow TS, et al. Exposure
525 of burrowing mammals to ²²²Rn. *Science of the Total Environment* 2012; 431: 252–261.
- 526 Berger MJ. Energy deposition in water by photons from point isotropic sources. *Journal of*
527 *Nuclear Medicine* 1968; 9: 15-25.
- 528 Berger MJ. Distribution of absorbed doses around point sources of electrons and beta particles
529 in water and other media. *Journal of Nuclear Medicine* 1971; 12: 5-23.
- 530 Bide RW, Armour SJ, Yee E. Allometric respiration/body mass data for animals to be used for
531 estimates of inhalation toxicity to young adult humans. *Journal of Applied Toxicology*
532 2000; 20: 273-290.
- 533 Brown J, Alfonso B, Avila R, Beresford N, Copplestone D, Hosseini A. A new version of the
534 ERICA tool to facilitate impact assessments of radioactivity on wild plants and animals.
535 *Journal of Environmental Radioactivity* 2016; 153: 141-149.
- 536 Brown JE, Alfonso B, Avila R, Beresford NA, Copplestone D, Pröhl G, et al. The ERICA Tool.
537 *Journal of Environmental Radioactivity* 2008; 99: 1371-1383.
- 538 Harley NH. Radon daughter dosimetry in the rat tracheobronchial tree. *Radiation Protection*
539 *Dosimetry* 1988; 24: 457-461.
- 540 Hofmann W, Crawford-Brown DJ, Fakir H, Monchaux G. Modelling lung cancer incidence in
541 rats following exposure to radon progeny. *Radiation Protection Dosimetry* 2006; 122:
542 345-348.
- 543 Hofmann W, Winkler-Heil R. From cellular doses to average lung dose. *Radiation Protection*
544 *Dosimetry* 2015; 167: 49-54.
- 545 ICRP. Radionuclide Transformations - Energy and Intensity of Transmissions. ICRP
546 Publication 38 (Annals of the ICRP 11), Pergamon Press, Oxford, 1983.
- 547 ICRP. Lung Cancer Risk from Exposures to Radon Daughters. ICRP Publication 50 (Annals of
548 the ICRP 17/1), Pergamon Press, Oxford, 1987.
- 549 ICRP. Protection Against Radon-222 at Home and at Work. International Commission on
550 Radiation Protection Publication 65. *Annals of the ICRP* 23 (2), 1993.
- 551 ICRP. Human respiratory tract model for radiological protection. (ICRP Publication 66. *Annals*
552 *of the ICRP* 24(1-3), International Commission on Radiological Protection, Elsevier
553 Science Ltd., Oxford, 1994.
- 554 ICRP. Guide for the Practical Application of the ICRP Human Respiratory Tract Model (ICRP
555 Publication SG3). *Annals of the ICRP* 32(1-2), International Commission on
556 Radiological Protection, Elsevier Science Ltd., Oxford, 2002.
- 557 ICRP. The 2007 Recommendations of the International Commission on Radiological
558 Protection. ICRP Publication 103, *Annals of the ICRP* 37 (2-4), Pergamon Press,
559 Oxford, 2007.
- 560 ICRP. The Concept and Use of Reference Animals and Plants for the Purposes of
561 Environmental Protection. J. Valentin (Ed.), International Commission on Radiological
562 Protection Publication 108, *Annals of the ICRP* 38(4-6), Elsevier, Oxford, 76 pp.,
563 2008a.
- 564 ICRP. Nuclear Decay Data for Dosimetric Calculations. International Commission on
565 Radiological Protection Publication 107. *Annals of the ICRP* 38 (3). 2008b.
- 566 ICRP. Lung Cancer Risk from Radon and Progeny and Statement on Radon. International
567 Commission on Radiation Protection Publication 115, *Annals of the ICRP* 40(1).
568 2010.
- 569 ICRP. Protection of the Environment under Different Exposure Situations. ICRP Publication
570 124, *Annals of the ICRP* 43(1). 2014a.

571 ICRP. Radiological Protection against Radon Exposure. International Commission on
572 Radiological Protection Publication 126. Ann. ICRP 43(3). 2014b.

573 ICRP. Dose Coefficients for Non-human Biota Environmentally Exposed to Radiation.
574 International Commission on Radiological Protection Publication 136 In press.

575 Keller G, Folkerts KH, Muth H. Special aspects of the Rn-222 and daughter product
576 concentrations in dwellings and in the open air. Radiation Protection Dosimetry 1984;
577 7: 151-154.

578 Kitowski I, Komosa A, Chodorowski J. Absorbed radiation dose from radon to the Sand Martin
579 Riparia riparia during breeding at the sand mines in eastern Poland. International Journal
580 of Environmental Research 2015; 9: 1097-1106.

581 Kleiber M. Body size and metabolism. Hilgardia 1932; 6: 315–351.

582 Kleiber M. Body size and metabolic rate. Physiological Reviews 1947; 27: 511–541.

583 Kojima H. The equilibrium factor between radon and its daughters in the lower atmosphere.
584 Environment International 1996; 22: S187-S192.

585 Kolokotronis T, Savage VM, Deeds EJ, Fontana W. Curvature in metabolic scaling. Nature
586 2010; 464: 753–756.

587 MacDonald CR, Laverock MJ. Radiation exposure and dose to small mammals in radon-rich
588 soils. Archives of Environmental Contamination and Toxicology 1998; 35: 109-120.

589 McWorter DB, Sunada DK. Groundwater Hydrology and Hydraulics, Water Resources
590 Publications, Fort Collins, Colorado, USA, 1988.

591 Porstendörfer J. Properties and behaviour of radon and thoron and their decay products in the
592 air. Journal of Aerosol Science 1994; 25: 219-263.

593 Reich PB, Tjoelker MB, Machado J-L, Oleksyn J. Universal scaling of respiratory metabolism,
594 size and nitrogen in plants. Nature 2005; 439: 457-461.

595 Rubner M. Über den Einfluss der Körpergrösse auf Stoff- und Kraftwechsel. Zeitschrift Fur
596 Biologie 1883; 19: 535-562.

597 Schmidt-Nielsen K. Scaling: Why is Animal Size So Important?: Cambridge University Press,
598 1984., 1984.

599 Strong JC, Baker ST. Lung deposition in rodents during exposure to attached radon progeny.
600 Environment International 1996; 22.

601 Taranenko V, Pröhl G, Gómez-Ros JM. Absorbed dose rate conversion coefficients for
602 reference biota for external photon and internal exposures. Journal of Radiological
603 Protection 2004; 24: A35–A62.

604 Tobias CA, Jones HB, Lawrence JH, Hamilton JG. The uptake and elimination of krypton and
605 other inert gases by the human body. Journal of Clinical Investigation 1949; 28: 1375–
606 1385.

607 Ulanovsky A. Absorbed doses in tissue-equivalent spheres above radioactive sources in soil.
608 Radiation and Environmental Biophysics 2014; 53: 729-737.

609 Ulanovsky A. Dosimetry for animals and plants: contending with biota diversity. Annals of the
610 ICRP 2016; 45: 225-238.

611 Ulanovsky A, Prohl G. A practical method for assessment of dose conversion coefficients for
612 aquatic biota. Radiation and Environmental Biophysics 2006; 45: 203-214.

613 Ulanovsky A, Prohl G. Dosimetry for Reference Animals and Plants: current state and
614 prospects. Annals of the ICRP 2012; 41: 218-232.

615 Ulanovsky A, Prohl G, Gomez-Ros JM. Methods for calculating dose conversion coefficients
616 for terrestrial and aquatic biota. Journal of Environmental Radioactivity 2008; 99: 1440-
617 1448.

618 Vives Batlle J, Jones SR, Copplestone D. A methodology for ^{41}Ar , $^{85,88}\text{Kr}$ and $^{131\text{m},133}\text{Xe}$ wildlife
619 dose assessment Journal of Environmental radioactivity 2015; 144: 152-161.

620 Vives i Batlle J, Coplestone D, Jones SR, Williams C. Allometric methodology for the
621 assessment of radon exposures to wildlife. *The Science of the Total Environment* 2012;
622 427-428: 50-59.

623 Vives i Batlle J, Jones SR, Coplestone D. Dosimetric model for biota exposure to inhaled
624 radon daughters. *Environment Agency Science Report SC060080*, 34 pp., 2008.

625 Vives i Batlle J, Jones SR, Gomez-Ros JM. A method for calculation of dose per unit
626 concentration values for aquatic biota. *Journal of Radiological Protection* 2004; 24:
627 A13-A34.

628 Vives i Batlle J, Smith AD, Vives-Lynch S, Coplestone D, Prohl G, Strand T. Model-derived
629 dose rates per unit concentration of radon in air in a generic plant geometry. *Radiation
630 and Environmental Biophysics* 2011; 50: 513-529.

631 Wenbin M, Yan J, Chanzhu Q, Weidao Z. Investigation of Indoor and Outdoor Radon and its
632 Daughters in the Region of Lianing, People's Republic of China. *Radiation Protection
633 Dosimetry* 1990; 30.

634 West GB, Brown JH. The origin of allometric scaling laws in biology from genomes to
635 ecosystems: Towards a quantitative unifying theory of biological structure and
636 organization. *Journal of Experimental Biology* 2005; 208: 1575 -1592.

637 Winkler-Heil R, Hussain M, Hofmann W. Stochastic rat lung dosimetry for inhaled radon
638 progeny: a surrogate for the human lung for lung cancer risk assessment. *Radiation and
639 Environmental Biophysics* 2015; 54: 225-241.

640 Wrixon AD, Green BMR, Lomas PR, Miles JCH, Cliff KD, Francis EA, et al. Natural radiation
641 exposure in UK dwellings. *National Radiological Protection Board Report NRPB R-
642 190*, Chilton, UK, 1988.

643